Are atmospheric-model tendency errors perceivable from routine observations?

Michael Tsyrulnikov[1] and Vadim Gorin[2]

1: HydroMetCenter of Russia
2: Massachusetts Institute of Technology

1 Abstract

In predictability experiments with simulated model errors (ME) and the COSMO model, reproducibility of ME from finite-time model-minus-observed tendencies is studied. It is found that in 1-h to 6-h tendencies, ME appear to be too heavily contaminated by noises due to, first, initial errors and, second, trajectory drift as a result of ME themselves. The resulting reproducibility error is far above the acceptable level. The conclusion is drawn that the accuracy and coverage of current routine observations are far from being sufficient to reliably estimate ME.

2 Introduction

ME (defined as tendency errors) are a very important source of forecast errors in meteorology. Both in ensemble prediction and ensemble data assimilation, ME need to be simulated according to their probability distribution (their spatio-temporal structure). However, very little is known to date on this subject. So, any objective knowledge on ME would be very helpful.

This study aims to advance our understanding of the ME structures in the atmosphere, including their spatio-temporal and cross-variable aspects. ME are intended here to be estimated using real observations, so that model tendencies can be confronted with observed tendencies. The first question — can ME be recovered from realistic finite-time model-tendencies vs. observed-tendencies? — is addressed in this note.

3 ME: the general paradigm

3.1 Definition of ME

We start with the forecast equation

$$\frac{\mathrm{d}X}{\mathrm{d}t} = F(X), \tag{1}$$

where $X = X^m$ is the model (forecast) state and F the model r.h.s. (model operator).

If we substitute the truth into Eq.(1), a discrepancy arises (because the model operator F is always not perfect) — this discrepancy is called the *model error*.

Otherwise stated, the ME is defined as the difference between the model tendency $F(X)$ (evaluated at the true system state!) and the true tendency (e.g. Orrell et al. 2001):

$$\varepsilon = F(X^t) - \frac{\mathrm{d}X^t}{\mathrm{d}t}, \tag{2}$$

where the superscript t denotes the truth.

Strictly speaking, X^t is the true system state *mapped to the model space*. To elaborate on this, we introduce a hypothetical *full* functional space, $\mathcal{X}_{full}$, where a 'full' system state X_{full} is defined and which includes more variables than the *model space* $\mathcal{X}$ (say, minor atmospheric gases, aerosols etc.) at much higher (maybe, infinite) resolution. We need this *full* space in order to be able to hypothesize the existence of a deterministic differential equation (like Eq.(1)) that governs the true atmospheric state (in the relatively small *model* space, we certainly cannot believe that such a deterministic equation for the truth exists):

$$\frac{\mathrm{d}X_{full}}{\mathrm{d}t} = F^t_{full}(X_{full}), \tag{3}$$

where $X_{full} \in \mathcal{X}_{full}$ and F^t_{full} is the hypothetical perfect full-space model operator.

We assume that the model space $\mathcal{X}$ is a subspace of the full space $\mathcal{X}_{full}$, with a projection $\mathcal{P}$ of $\mathcal{X}_{full}$ onto $\mathcal{X}$: $X = \mathcal{P}X_{full}$.

Next, we apply the projection operator $\mathcal{P}$ to Eq.(3), getting

$$\frac{\mathrm{d}X}{\mathrm{d}t} = \mathcal{P}F^t_{full}(X_{full}) =: F^t(X_{full}). \tag{4}$$

So, the model-space state vector X (any state vector, not just the true one) satisfies:

$$\frac{\mathrm{d}X}{\mathrm{d}t} = F^t(X_{full}). \tag{5}$$

Now, we have both the model tendency $F(X)$ and the true tendency $F^t(X_{full})$, so that the ME can be defined as their difference:

$$\varepsilon = F(X) - F^t(X_{full}), \tag{6}$$

where $X = \mathcal{P}X_{full}$.

From Eq.(6), it follows that ε is a function of the point in *full* space: $\varepsilon = \varepsilon(X_{full})$ (in other words, ε in *defined* on $\mathcal{X}_{full}$).

Note that this second definition of ME given by Eq.(6) is, in a sense, more general than the usual definition given by Eq.(2). Indeed, Eq.(2) defines ME only at an actual true system state X^t, whereas Eq.(6) defines ME at any point in full space. This more general definition may be helpful in understanding the nature of ME and can be used in practice if an approximation to the true model $F^t(X_{full})$ is available.

We conclude the definitions subsection by remarking that the above ME are defined as *additive*: $\varepsilon = \varepsilon_{add} = F - F^t$. In principle, one could define them as multiplicative or in some other way.

3.2 How to evaluate ME?

Apparently, Eq.(6) can be useful in evaluating ε only if the true model-space operator $F^t(X_{full})$ is available. If not, we have to use the ME definition Eq.(2) and rely on the *observed truth* $X^t|_{obs}$ (not the *full* truth X^t_{full} and even not the model-space truth X^t!): e.g., we may expect that horizontal winds or temperature are observed, whereas vertical wind is not, etc.

Assuming $X^t|_{obs}$ is available for some period of time and aiming to evaluate ε, we use Eq.(2) evaluated at $X = X^t|_{obs}$:

$$\varepsilon|_{obs} = F|_{obs}(X^t) - \frac{\mathrm{d}X^t|_{obs}}{\mathrm{d}t}. \tag{7}$$

Here and elsewhere, $|_{obs}$ denotes restriction to *observed* space $\mathcal{X}|_{obs}$: $X|_{obs} = \Pi X$, where Π is the suitable projection (spatial interpolation to observation points).

Note that the standard definition of ME, Eq.(2), can be regarded as a particular case of Eq.(7) when the entire X^t is observed. Normally, X^t is *not* completely observed, so our basic equation in ME estimation will be Eq.(7).

It is worth stressing at this point that in Eq.(7), the argument of $F|_{obs}$ is the *model-space* (not observed-space!) X^t, which is only partially observed. This is the first major obstacle in objective ME evaluation/estimation: given the partially observed truth, $X^t|_{obs}$, we cannot exactly evaluate ε and so approximations are indispensable. In the predictability theory language, lack of X^t knowledge is nothing other than the error in initial conditions (analysis error). The other major obstacle — finite-time-tendency approximations — is discussed below.

We conclude this subsection by reiterating that we have defined the hierarchy of three embedded phase spaces:

1. The largest (hypothetical) *full* space $\mathcal{X}_{full}$, where the *true* system equation operates.
2. The medium (forecast) *model* space $\mathcal{X}$, where the *forecast* equation (the forecst model) is defined, $\mathcal{X} = \mathcal{P}\mathcal{X}_{full}$.
3. The smallest *observed* space $\mathcal{X}|_{obs}$, which consists of those model-space points that can be *observed*, $\mathcal{X}_{obs} = \Pi\mathcal{X}$.

3.3 Stochastic modelling of ME

From Eq.(6), we see that ME is some (unknown and, presumably, very complicated) function of the 'full' system state X_{full}. In reality, the 'full' system state is not just huge but even unknown, so that given some X, we are unable to recover $F^t(X_{full})$ not only because F^t is unknown but also because X_{full} is unavailable. This leads us to model the ME stochastically.

4 Finite-time ME

As only finite-time tendencies are observable in real world, we turn to time-integrated tendencies and ME.

If we regard system (model) state as an element of the respective functional (or, in the spatially discrete case, Euclidean) space, then Eq.(7) is nothing other than an ordinary differential equation. Therefore, we are allowed to integrate it in time from t_0 to $t_0 + \Delta t$, getting:

$$\breve{\varepsilon} := \int \varepsilon \, \mathrm{d}t = \int F(X^t) \, \mathrm{d}t - \Delta X^t, \tag{8}$$

where Δf denotes, for any function f, the temporal finite difference $\Delta f = f(t_0 + \Delta t) - f(t_0)$ and $\breve{f}$ stands for time integrated f: $\breve{f} = \int_{t_0}^{t_0+\Delta t} f(t) \, \mathrm{d}t$ [mnemonics: $\breve{}$ is reminiscent of an *accumulation* device]. Note that $\breve{\varepsilon}$ is sometimes called the *drift* (e.g. Orrell et al. 2001).

In Eq.(8), ΔX^t is available through observations (up to an observation error with known probability distribution); the unavailable quantity $F(X^t)$ can be approximated by the best available one, $F(X^m)$, where X^m is the model forecast started from an analysis. The replacement $X^t \to X^m$ gives rise to the error

$$\delta := \int F(X^m) \, \mathrm{d}t - \int F(X^t) \, \mathrm{d}t, \tag{9}$$

so that, since $\int F(X^m)\,\mathrm{d}t = \Delta X^m$, we have

$$\breve{\varepsilon} = \Delta X^m - \Delta X^t - \delta. \tag{10}$$

The error term δ appears due to, first, the initial-conditions difference ($X^m(t_0)$ differs from $X^t(t_0)$) and second, due to the drift of the model trajectory from the true one — provided both trajectories start from the same initial conditions. Indeed, denote by $X^{mt}(t)$ the (phase-space) *model* trajectory started from *true* initial conditions, see Fig.1.

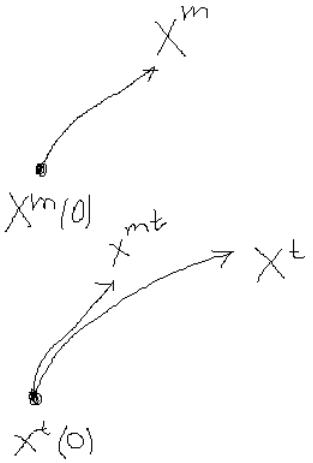

Figure 1: Model forecast X^m, the truth X^t, and the model forecast X^{mt} started from true initial conditions.

We may rewrite Eq.(9) as

$$\delta = \int [F(X^m) - F(X^{mt})]\,\mathrm{d}t + \int [F(X^{mt}) - F(X^t)]\,\mathrm{d}t. \tag{11}$$

Here, the first integral,

$$\delta_{ie} := \int [F(X^m) - F(X^{mt})]\,\mathrm{d}t. \tag{12}$$

is purely due to the forecast error growth in response to the initial error (the *internal* error growth, see e.g. Reynolds et al. 1994). The second integral,

$$\delta_{me} := \int [F(X^{mt}) - F(X^t)]\,\mathrm{d}t. \tag{13}$$

does not contain any contribution from the initial error $X^m(t_0) - X^t(t_0)$ and is solely due to ME (the *external* error growth, Reynolds et al. 1994).

In the Appendix, it is shown that for very small tendency interval lengths Δt, δ_{me} can be neglected: $\delta_{me} \ll \breve{\varepsilon}$. But experimentally, we found that in order for δ_{me} to be really negligible, Δt needs to be as small as 1 h (!) for winds and about 6 h for temperature (see below the numerical experiments section).

In general, both terms should be retained:

$$\breve{\varepsilon} = \Delta X^m - \Delta X^t - \delta_{ie} - \delta_{me}. \tag{14}$$

In the realistic situation, when the truth is available through noisy observations $X^o = X^t + \eta$, where η is the observation error, ΔX^t should be replaced in this equation by the *observed* tendency, ΔX^o:

$$\breve{\varepsilon} = \Delta X^m - \Delta X^o - \delta_{ie} - \delta_{me} - \Delta\eta. \tag{15}$$

The accumulated ME $\breve{\varepsilon}$ can only be seen in the observable $\Delta X^m - \Delta X^o$ difference if the noise terms δ_{ie}, δ_{me}, and $\Delta\eta$ in Eq.(15) are small enough. This, again, is will be checked in numerical experiments, see below. In principle, the 'signal' $\breve{\varepsilon}$ can be extracted from the difference $\Delta X^m - \Delta X^o$ not only if the noise is small but also if the noise has very well known probabilistic distribution. But this does not seem to be case in this problem: only the observation noise can be assumed to have more or less known distribution. The analysis error δ_{ie} and the model-error finite-time distortion δ_{me} are too poorly known. So, all we can hope is to find that the noise is small — compared with the forecast tendency (or the observed tendency).

5 Numerical predictability experiments

5.1 Goals

Using predictability experiments with known *a priori* ('synthetic') ME, find out whether the ME can be recovered (estimated) from forecast and observed (Eulerian) tendencies. In particular, assess the roles of the noise sources, δ_{ie} and δ_{me}, which contaminate the finite-time ME, $\breve{\varepsilon}$, as functions of observation-error variance, model-error variance, and the length of the finite-time tendency Δt.

5.2 The forecast model

COSMO model version 4.13 is used. The model grid has 40 full levels (41 half levels), 14 km mesh size in the horizontal, and has the top at about 40 hPa. The domain is European Russia (about 4500 by 5000 km).

5.3 Methodology

In the most general terms, we mimic the intermittent data assimilation cycle with "synthetic" observations and ME model (MEM), so that the observation-error statistics (variance) and ME themselves are known *a priori*.

5.3.1 Model errors

We assume here that only temperature and horizontal winds forecast equations are in error. We employ the simplest non-degenerate MEM: for each of the fields T, u, and v, the respective ε are specified to be *additive and constant in space and time during one assimilation cycle* (6 h). At different assimilation cycles (6-h intervals) ε are mutually independent zero-mean Gaussian pseudo-random variables with pre-specified variance σ_ε^2.

Thus, σ_ε is the only parameter of MEM for each of the three fields: T, u, v.

It is worth stressing that this MEM is not only the simplest one but also the one which can be most easily estimated. So, we simplified the MEM estimation problem to the greatest sensible extent. Our intention here is to try to solve the simplest problem, so that if we fail, there will be no sense to tackle the problem in a more realistic setup.

5.3.2 The 'truth'

The truth run is accomplished by time integration of the perturbed COSMO model: at each model time step, ε is subtracted from the r.h.s. of the model equations following the equation for the truth,

$$\frac{\mathrm{d}X^t}{\mathrm{d}t} = F(X^t) - \varepsilon. \tag{16}$$

(see Eqs.(7) and (2)).

The upper and lateral boundary conditions are exactly the same as for the model forecast (see below).

5.3.3 Observations

We assume that every degree of freedom in the fields T, u, v, q is observed — subject to observation error η.

In order to make the analysis (described below is this section) as simple as possible, we impose the observation error field that has, roughly, the same covariances as analysis background (6-h forecast) error covariances. Aiming at decorrelation length scales of about 100 km in the horizontal and 100 hPa in the vertical, we employ the following technique.

First, at the *thinned* COSMO grid (in the below experiments, we take every 5th grid point in the horizontal and every or 3rd grid point in the vertical), we simulate white noise with some variance σ^2_{ini} subject to subsequent tuning.

Second, we tri-linearly interpolate the observation-error field from the thinned grid to the full grid.

Third, we apply, several times, a smoothing filter (a moving average operator), which is defined as a simple averaging over the $5 \times 5 \times 3$ cube on the grid (5×5 in the horizontal and 3 in the vertical) on the COSMO grid. The more smoothing sweeps, the smoother the resulting field. There is also a minimum number of sweeps needed to make the field homogeneous (so that points on the thinned grid are no longer distinguishable from other grid points in the simulated fields).

For the selected number of sweeps (5 sweeps are used in the experiments described below), the variance σ_{ini} is finally tuned to yield the desired observation-error variance $\sigma^2|_{obs}$.

A realization of the pseudo-random observation-noise field is displayed in Fig.2 (a horizontal cross-section) and Fig.3 (a vertical cross-section).

5.3.4 Analysis

The analysis is univariate for all 4 fields (T, u, v, q). Since observations are placed at all grid points, the observation operator is the identity matrix for each univariate analysis: $H = I$. So, the gain matrix becomes

$$K = B(B + R)^{-1}. \tag{17}$$

As noted above, we assume the proportionality $R \propto B$, so that Eq.(17) rewrites as

$$K = \frac{\sigma_b^2}{\sigma_b^2 + \sigma_{obs}^2} \cdot I, \tag{18}$$

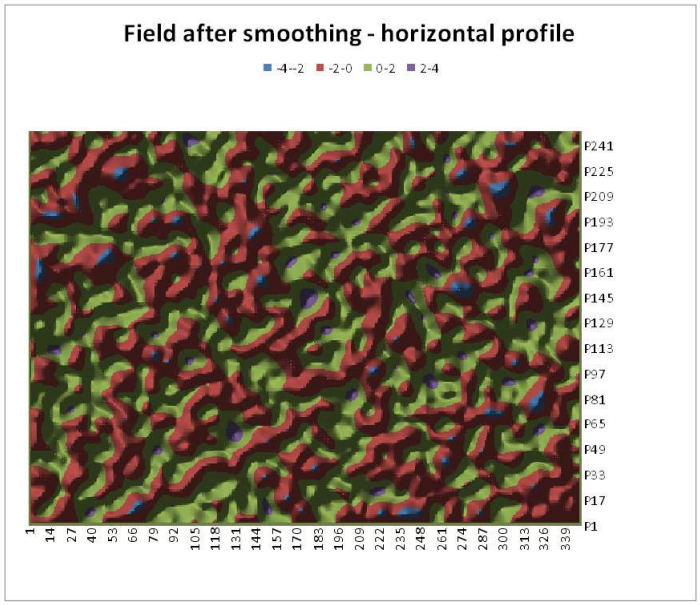

Figure 2: A horizontal cross-section of the observation noise.

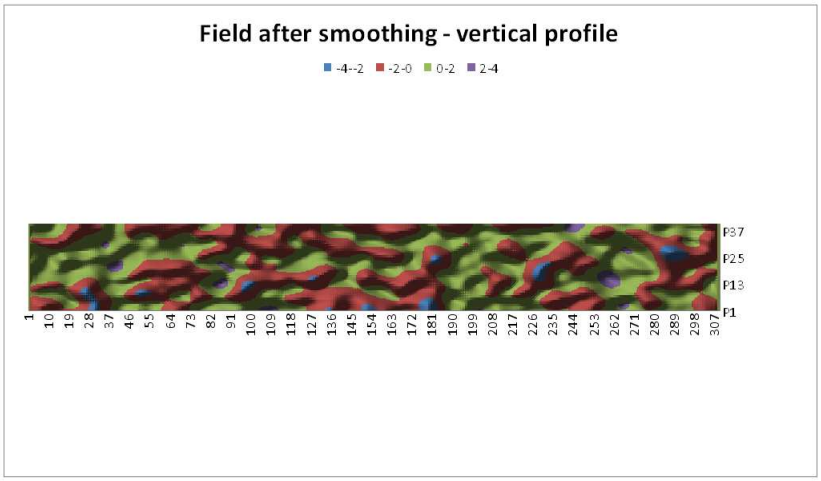

Figure 3: A vertical cross-section of the observation noise.

where σ_b is the background-error standard deviation and σ_{obs} the observation-error standard deviation.

This implies that the analysis decouples into a series of scalar (grid-point-wise) analyses. So, the analysis scheme is here extremely simple and fast.

After T, u, v, q fields are analyzed, we compute the p field by integrating the hydrostatic equation starting from the top model level, where COSMO is coupled with the global driving model. All computations are performed on the native COSMO grids.

5.3.5 Forecast

6-h forecasts at each assimilation cycle start from the above analyses and are performed with the unperturbed COSMO model — exactly as in the real world. The upper and lateral boundary conditions are build from the sequence of global driving-model analyses and 3-h forecasts with linear interpolation within 3-h time intervals.

5.4 Estimation of instantaneous ME from finite-time forecast-minus-observed tendencies. The experimental setup

Finite-time ME in T, u, v are checked. The length of the finite-time tendency Δt ranges from 1 h to 6 h. Recall that the ME are constant in space and time: within one cycle in the assimilation mode and for the whole forecast in the forecast mode.

ME temperature and wind components standard deviations are set up to be on two levels: realistic (1 K per day for T and 2 m/s per day for u and v) and unrealistically high (5 times larger: 5 K per day and 10 m/s per day, respectively).

Observation error standard deviations are set up again on two levels: realistic (1 K and 2 m/s for temperature and each of the two wind components, respectively) and unrealistically low (0.1 K for T and 0.2 m/s for u and v).

The intention with specifying unrealistically large ME and unrealistically low observation errors was to seek the condition under which ME *can be* estimated using observations.

5.5 ME observability criterion

Equation (15) shows that finite-time ME $\breve{\varepsilon}$ is observable through the difference of finite-time model tendencies and observed tendencies if

$$\breve{\varepsilon} \approx \Delta X^m - \Delta X^o. \tag{19}$$

We measure the degree of error involved in this approximate equality by the relative error defined as

$$r := \frac{\|\Delta X^m - \Delta X^o - \breve{\varepsilon}\|}{\|\breve{\varepsilon}\|}. \tag{20}$$

The norm here is the standard L^2 norm, where involves averaging over the central third of the domain in each of the three spatial dimensions and over assimilation cycles.

With our constant imposed ME $\varepsilon = \varepsilon_0$, the dift $\breve{\varepsilon}$ is simply $\breve{\varepsilon} = \varepsilon_0 \cdot \Delta t$.

Thus, for all assimilation experiments, we calculate r and, if $r \leq 0.3$, we conclude that ME is observable and if $r > 0.3$ ME is not observable.

We check the three forecast tendency lengths $\Delta t = 1$, 3, and 6 h.

5.6 Results: Assessment of the ME observability errors

With the above realistic both ME and observation errors, the ME relative observability error r (see Eq.(20)) appears to be unacceptably high for all three tendency lengths examined: 1, 3, and 6 h. So, we don't display those results and turn to less realistic setups with better ME observability (smaller observation errors and/or larger ME).

Table 1 shows the values of r for the *unrealistic* case when observation errors are set to the very small levels: 0.1 K for temperature and 0.2 m/s for each wind component. Note that for technical reasons, in this and the next table, some cells are not filled in. We believe the presented results are quite enough to judge whether the selected ME estimation approach is viable.

Specifically, from Table 1, we see that even for unrealistically small observation errors (OE) and despite all degrees of freedom are observed for the four fields (T, u, v, q), the relative ME observability errors r are unacceptably high (see the first horizontal data section "OE small" in Table 1).

Table 1: RMS relative errors of ME observability. The unrealistic case (observation errors are small or zero; ME are realistic)

OE	Field	$\Delta t = 1$ h	$\Delta t = 3$ h	$\Delta t = 6$ h
OE small	T	> 1		0.68
	u	> 1		2.7
	v	> 1		3.4
OE=0	T	1.0	0.58	0.46
	u	1.2	1.8	1.6
	v	1.4	1.5	2.0
Fc starts	T	0.28	0.30	0.33
from	u	0.33	0.75	0.99
truth	v	0.35	0.69	1.20

The second horizontal data section in Table 1 (OE=0) presents the values of r for the case when observations (both in the assimilated observations and the observations used to compute the observed tendencies ΔX^o) are perfect. In this case, the observability error stems from, first, initial errors in the unobserved fields, second, from errors in the hydrostatically recovered pressure field, and third, from the ME-induced trajectory drift effect, δ_{me}. We see that even for perfect observations, r never becomes acceptable (i.e. is never less than $r = 0.3$) for neither of the three fields (T, u, v) and neither of the three tendency lengths (1, 3, 6 h).

Three points are worth noting here. First, T appears to be less badly observable than both u and v. This is discussed in the Interpretation section below. Second, for winds, r increases with the increasing Δt. Third, for temperature, the reverse Δt dependence occurs. This latter outcome can be assigned to the absence of wind-mass balancing in our simplistic analysis.

The lowermost horizontal data section of Table 1 corresponds to the setup in which no assimilation is, in fact, present and the forecasts start directly from the 'truth'. In this case, the ME observability error is caused only by the δ_{me} error component. We see that here, *temperature* ME observability errors are close to acceptable for all Δt, whereas *wind* ME errors are nearly acceptable only for $\Delta t = 1$ h. An interpretation of this difference in observability between temperature and winds will be given below in section .

Next, we examine the *extremely unrealistic* case — when OE are unrealistically low (or absent) whereas ME are unrealistically high, see Table 2. Qualitatively, the results here are largely the same as those presented in Table 1. This implies that nonlinearity does not play a significant role in ME observability in finite-time tendencies.

Further, we present typical plots of forecast-minus-observed tendencies $(\Delta X^m(t) - \Delta X^o(t))$ as well as expected tendencies $(\varepsilon_0 \cdot (t - t_0))$ as functions of lead time t. We consider here the case when forecasts start from the 'truth', so that only the δ_{me} error component plays a role here. Note that we show the plots for an arbitrarily selected grid point and at an arbitrary cycle of our intermittent data assimilation with "synthetic" observations.

Fig. 4 shows that for T, with perfect initial conditions, the 'target' $\varepsilon_0 \cdot (t - t_0)$ finite-time tendency error is roughly reproduced, albeit with an error, for the lead times up to about 12 h. Fig. 5 demonstrates that the u-wind ME observability time span is not longer than 2 h. As for the v-wind, the ME turn out to be observable during a period of time as short as about 1 h (see Fig. 6).

Next, we note that we have checked different ME amplitudes and found (somewhat sur-

Table 2: RMS relative errors of ME observability. The extremely unrealistic case (observation errors are small or zero; ME are unrealistically high)

OE	Field	$\Delta t = 1$ h	$\Delta t = 3$ h	$\Delta t = 6$ h
OE small	T	0.80	0.41	0.35
	u	1.75	0.98	1.09
	v	2.26	1.38	1.42
OE=0	T			0.34
	u			1.02
	v			1.30
Fc starts	T	0.27		0.34
from	u	0.26		0.98
truth	v	0.34		1.26

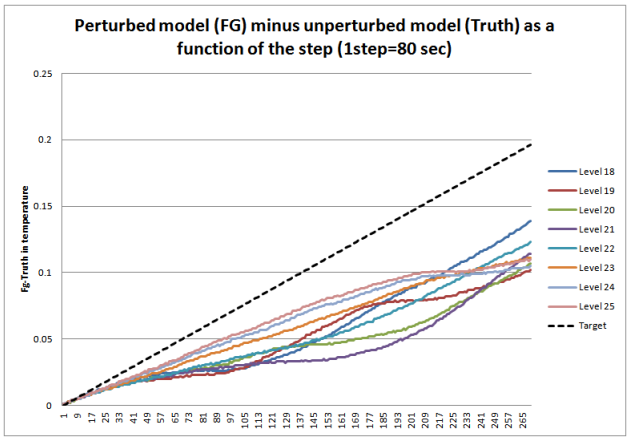

Figure 4: Forecast tendency T errors at different model levels vs. the integrated ME (dashed) at an arbitrary grid point

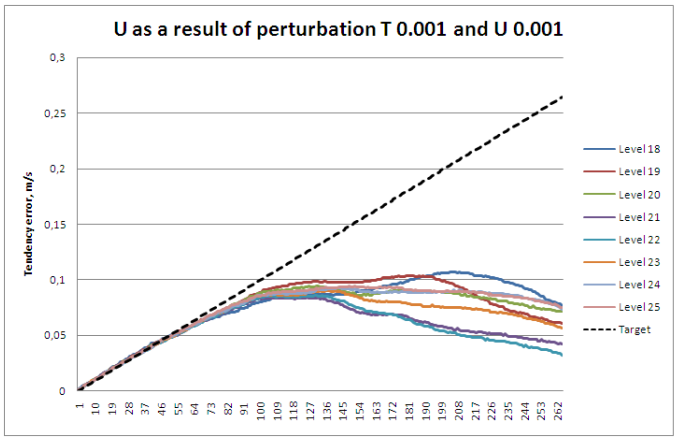

Figure 5: Same as Fig.4 except for u.

prisingly) that the ME observability does not depend much on the ME amplitude. This is confirmed by the relative errors presented in the lowermost horizontal sections of tables 1 and 2. So, linear mixing of the flow seems to be of primary importance, not its non-linearity.

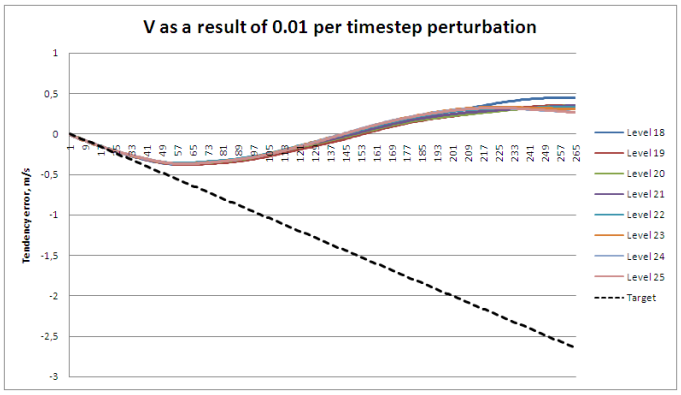

Figure 6: Same as Fig.4 except for v.

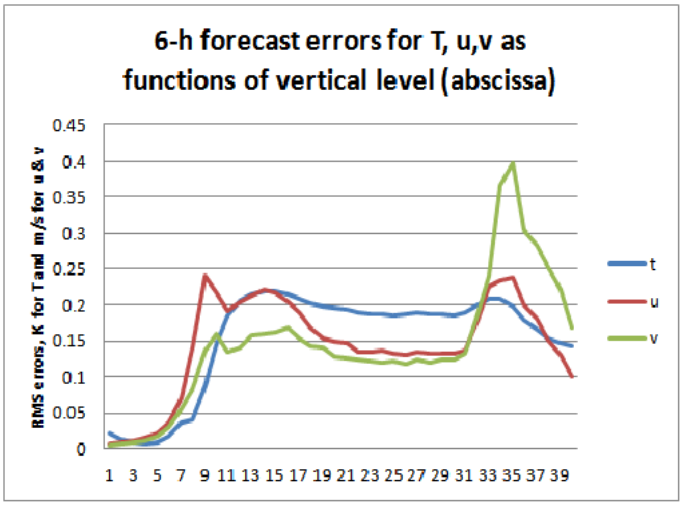

Figure 7: 6-h forecast RMS errors due to ME as functions of the vertical model level (realistic ME).

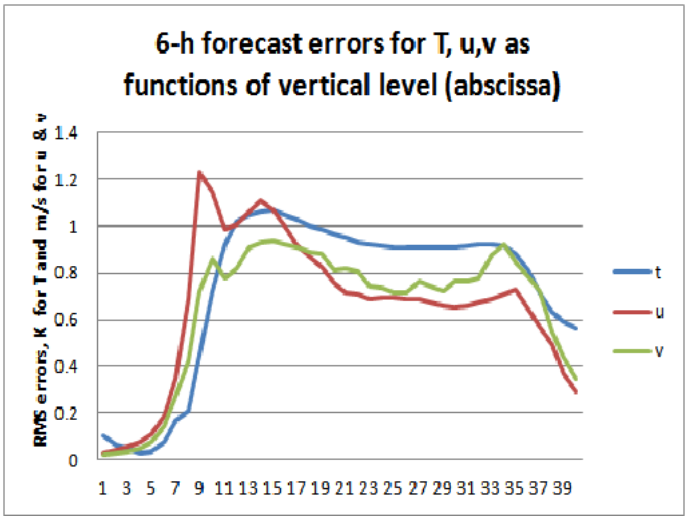

Figure 8: 6-h forecast RMS errors due to ME as functions of the vertical model level (unrealistically high ME).

Finally, we display standard deviations of the ME-induced forecast errors themselves (the

forecasts start from the 'truth' and last for 6 h) as functions of altitude. Figs. 7 and 8 show that near the boundaries, especially near the upper boundary, the impact of ME is significantly reduced. This implies that introducing perturbations into boundary conditions is inevitable if we wish to obtain realistic forecast ensemble spread within the whole model atmosphere. The same conclusion is certainly valid for the lateral boundaries (not checked).

5.7 Conclusions drawn from the experiments

With the existing level of observation errors and ME, even the perfect observational coverage does not allow us to perceive the imposed most easily estimable constant-ME in finite-time forecast tendencies. The noise from initial errors (including the unobserved fields, like hydrometeors and vertical wind) and from the ME-induced trajectory drift (mixing the ME signal with the fields themselves) appears to be too high for the tested ME estimation approach to be useful.

5.8 Interpretation of the experimental results

Here, we discuss, using simple models, why for winds, ME disappear in the forecast tendency errors much more quickly than for temperature. We also check whether it is worth switching from Eulerian to Lagrangean tendencies in our ME estimation attempts.

The aim of this section is to theoretically verify that the above experimental results are, at least qualitatively, meaningful. This will make our conclusions more credible. Without any theoretical analysis, we would be less confident that the results of the experiments are really relevant for the problem at hand and are not caused by a program bug or other artifacts.

5.8.1 Temperature ME

Let the forecast model be the 1-D advection equation with a pre-specified and exactly known advection velocity c:

$$T^m_t + cT^m_x = 0, \tag{21}$$

where subscripts t and x stand for time and space partial derivatives, respectively, and the superscript m means "model" (forecast).

The 'truth' is, in accord with Eq.(2),

$$T^t_t + cT^t_x = -\varepsilon, \tag{22}$$

where the superscript t means the 'truth".

Let, further, the model (forecast) starts, at $t = t_0$, from the 'truth'. Then, the forecast-error (i.e. $T' := T^m - T^t$) equation, obtained by subtraction of Eq.(22) from Eq.(21), satisfies the following equation

$$T'_t + cT'_x = \varepsilon, \tag{23}$$

with the initial condition

$$T'(t_0) = 0. \tag{24}$$

Knowing $c = c(t, x)$, we easily solve the initial problem Eq.(23)–(24) using the method of characteristics:

$$\frac{\mathrm{d}T'}{\mathrm{d}t} = \varepsilon, \tag{25}$$

where $\dot{/}\mathrm{d}t$ denotes the full derivative along the physical-space trajectory defined by the equation

$$\frac{\mathrm{d}x}{\mathrm{d}t} = c(t,x) \tag{26}$$

and the initial condition

$$x(t_0) = x_0. \tag{27}$$

Integrating Eq.(25) along the advection trajectory (the characteristic) yields (recall, for zero initial error T')

$$T'(t,x) = \int_{t_0}^{t} \varepsilon(t, x(t,x_0))\,\mathrm{d}t \equiv \breve{\varepsilon}. \tag{28}$$

For constant in space and time ε, Eq.(28) implies that the forecast tendency error *does reproduce* $\breve{\varepsilon}$. This is in concert with the above experimental result: temperature ME are better observable from finite-time tendency errors than wind ME. Now, let us turn to the latter.

5.8.2 Wind

The principal difference from the temperature case it that wind is both the advected quantity and the advection velocity itself. Therefore, let us consider the non-linear advection equation (again, in 1-D) for the u wind component:

$$u^m_t + u^m u^m_x = 0, \tag{29}$$

$$u^t_t + u^t u^t_x = -\varepsilon. \tag{30}$$

Expressing $u^t = u^m - u'$, subtracting Eq.(30) from Eq. (29), and neglecting, for simplicity of the analysis, the non-linear (w.r.t. the perturbation u') term $u'u'_x$, we obtain

$$u'_t + u^m u'_x + u' u^m_x = \varepsilon \tag{31}$$

or, rearranging the terms,

$$u'_t + u^m u'_x = -u' u^m_x + \varepsilon. \tag{32}$$

Comparing this equation with its counterpart for temperature, Eq. (23), we see one single qualitative difference: the presence of the term $(-u'u^m_x)$ in the r.h.s. of the equation. To understand how it impacts the solution, let us suppose that $u^m_x \equiv g = const$ (i.e. u^m is a linear function of x only). Then, we have

$$\frac{\mathrm{d}u'}{\mathrm{d}t} = -gu' + \varepsilon. \tag{33}$$

Here, as before for temperature, $\mathrm{d}/\mathrm{d}t$ denotes the full derivative along the physical-space trajectory defined by the equation

$$\frac{\mathrm{d}x}{\mathrm{d}t} = u^m. \tag{34}$$

Along any trajectory defined by Eq.(34), with zero initial condition $u'(t=0) = 0$, Eq.(33) is easily solved:

$$u'(t, x(t,x_0)) = \exp(-gt) \int_{t_0}^{t} \exp(g\tau)\varepsilon(\tau, x(\tau, x_0))\mathrm{d}\tau. \tag{35}$$

In this equation, the important feature is that in the course of integration, ε is multiplied by $\exp(g\tau)$, i.e. ε is *distorted*. This distortion makes the finite-time forecast tendency error

less and less related to the integrated ME. We may, thus, speculate that it is this effect that makes *wind* ME less observable than temperature ME.

As a final remark here, we note that Eq.(35) implies that the ME observability time scale can be assessed as $g^{-1} = (u_x^m)^{-1}$, the flow time scale. For meso-scale flows, this time scale is of the order of hours, and so is, thus, the ME observability time.

5.8.3 Lagrangean vs. Eulerian tendencies

Let us consider the temperature advection equation, Eq.(21), and assume, in contrast to Eq.(22), that temperature ME is due to mis-specified advection velocity c as well as due to the temperature ME:

$$c \equiv c^m = c^t + c' : \tag{36}$$

$$T_t^m + c^m T_x^m = 0 \tag{37}$$

$$T_t^t + c^t T_x^t = -\varepsilon \tag{38}$$

$$T^m = T^t + T'. \tag{39}$$

Expressing $c^t = c^m - c'$ and $T^t = T^m - T'$, substituting them into Eq.(38) and subtracting the resulting equation from Eq.(37) yields:

$$T'_t + c^m T'_x + c' T_x^m - c' T'_x = \varepsilon. \tag{40}$$

In this equation, with the *Eulerian* tendency, T'_t, is contaminated by the three terms: $c^m T'_x + c' T_x^m - c' T'_x$, whereas with the *Largangean* tendency, $T'_t + c^m T'_x$, only by the two terms: $c' T_x^m - c' T'_x$. Now, we claim that the difference between the two cases is not dramatic. Indeed, the 'gain' $c^m T'_x$ is comparable in magnitude with one remaining term, $c' T_x^m$. This can be seen by assuming realistic wind and temperature errors, and realistic natural variability standard deviations and length scales (not shown).

So, we conclude that, although switching from Eulerian to Lagrangean tendencies can reduce the impact of forecast errors due to initial errors propagated by advection, the contamination of the finite-time tendency errors by the ME-induced trajectory drift can hardly be reduced.

We note here that, in addition, advection error propagation is only part of the initial-error evolution. Further, in the above analysis, we did not take in to account the vertical advection associated with much larger errors in w. Finally, we do not have a dense enough in-situ observation network to estimate the Lagrangean tendencies (using remote sensing data is doubtful in view of their possible spatially and temporally correlated observation errors).

Summarizing this Eulerian/Lagrangean subsubsection, turning to Lagrangean tendencies would imply only a minor improvement and thus is not worth trying.

Summarizing the interpretational subsection , we conclude that the experimental results do not contradict to the theoretical conclusions/speculations.

Summarizing the whole experimental section, we conclude that the observation-based ME estimation endeavor has failed. This failure is confirmed by theoretic considerations.

6 Conclusions

The above experimental results unequivocally imply that perceivable (through in-situ observations) finite-time tendency errors are too heavily contaminated by both initial errors and

ME-induced trajectory drift errors, so that the signal-to-noise ratio is well below 1. Without having, thus, any real access to (time-integrated) true ME, any estimator that uses the difference between the model tendency and the observed tendency as a proxy to the true ME, would inevitably fail. In principle, one can imagine a much more sophisticated approach that attempts to allow for the (stochastic) distortion of ME by the chaotic atmosphere flow. But a realization of such an approach would be very difficult and time consuming, without any guarantee of success.

It is worth stressing that not only *instantaneous* ME are not recoverable from finite-time forecast-minus-observed tendencies, but *finite-time* ME are not recoverable either. Indeed, in our experiments we imposed constant in space and time ME.

So, with existing routine observations, an observations based ME estimation technique appears to be not feasible.

Appendix. Assessment of the ε-induced trajectory drift

Here, we wish to understand whether or not the quantity

$$\delta_{me} := \int_{t_0}^{t_0+\Delta t} F(X^{mt})dt - \int_{t_0}^{t_0+\Delta t} F(X^{t})dt \tag{41}$$

(where the model forecast X^{mt} starts from the truth, $X^{mt}(t_0) = X^t(t_0)$) can be neglected in comparison with the time integrated ME:

$$\breve{\varepsilon} := \int_{t_0}^{t_0+\Delta t} \varepsilon(t)\,\mathrm{d}t. \tag{42}$$

To set up the problem, we, first, suppose that Δt is small enough for $X^{mt}(t)$ to remain close to $X^t(t)$ in the sense that the first-order Taylor expansion around X^{mt} can be applied:

$$F(X^t) = F(X^{mt}) - A \cdot \delta X, \tag{43}$$

where A is the Jacobian $\partial F/\partial X$ and

$$\delta X := X^{mt} - X^t. \tag{44}$$

Next, for simplicity of the analysis, we postulate that the operator A in Eq.(43) can be taken constant within $t \in (t_0, t_0 + \Delta t)$. Then the discrepancy δ_{me} becomes

$$\delta_{me} = \int_{t_0}^{t_0+\Delta t} A \cdot \delta X(t)\,\mathrm{d}t = A \int_{t_0}^{t_0+\Delta t} \delta X(t)\,\mathrm{d}t. \tag{45}$$

Now, we find $\delta X(t)$. From

$$\frac{dX^{mt}}{dt} = F(X^{mt}) \tag{46}$$

and

$$\frac{dX^{t}}{dt} = F(X^{t}) - \varepsilon, \tag{47}$$

we see that δX satisfies the equation

$$\frac{d\delta X}{dt} = A \cdot \delta X + \varepsilon \tag{48}$$

supplemented with the initial condition $\delta X(t_0) = 0$.

It is easy to show that the solution to Eq.(48) with zero initial condition is

$$\delta X(t) = \exp(At) \int_{t_0}^{t_0+\Delta t} \exp^{(} -As)\varepsilon(s)\,\mathrm{d}s. \tag{49}$$

Now, we return to the discrepancy in question, δ_{me}, and substitute $\delta X(t)$ from Eq.(48) into Eq.(45):

$$\delta_{me} = A \int_{t_0}^{t_0+\Delta t} \exp(At)dt \int_{t_0}^{t_0+\Delta t} \exp(-As)\varepsilon(s)\,\mathrm{d}s. \tag{50}$$

Let us evaluate Eq.(50) in the asymptotic limit $\Delta t \to 0$. For small enough Δt, $\varepsilon(s) \sim \varepsilon(t_0) \equiv \varepsilon_0$ and $\exp(At) \sim I + A(t - t_0)$, so that

$$\delta_{me} \sim A\varepsilon_0 \Delta t^2. \tag{51}$$

We roughly assess the application of A as multiplication by its time scale (the dynamical time scale T_{dyn}), thus Eq.(51) becomes

$$\delta_{me} \sim \varepsilon_0 \frac{\Delta t^2}{T_{dyn}}. \tag{52}$$

We note that the discrepancy r is important if it's comparable with $\breve{\varepsilon} \approx \varepsilon_0 \Delta t$. We see that the 'noise-to-signal ratio' is

$$\frac{\delta_{me}}{\breve{\varepsilon}} \approx \frac{\Delta t}{T_{dyn}}. \tag{53}$$

This equation suggests that we are allowed to neglect δ_{me} if $\Delta t \ll T_{dyn}$. On the meso scale, with T_{dyn} as small as hours, the 12-h tendencies appear to fail to capture the ME structure. Δt needs to be very small, perhaps, of the order of 1 h or less.

References

[1] Orrell, D., Smith, L., Barkmeijer, J., and T.N.Palmer, 2001: Model error in weather forecasting. *Nonlinear Processes in Geophysics*, v.8, **357-371**.

[2] Reynolds, C.A., Webster, P.J. and E. Kalnay, 1994: Random error growth in NMC's global forecasts. *Mon. Wea. Rev.*, v. 122, **1281-1305**.